

UC Riverside

UC Riverside Previously Published Works

Title

Identifying Planetary Biosignature Impostors: Spectral Features of CO and O₄ Resulting from Abiotic O₂/O₃ Production

Permalink

<https://escholarship.org/uc/item/638094n8>

Authors

Schwieterman, Edward W
Meadows, Victoria S
Domagal-Goldman, Shawn D
[et al.](#)

Publication Date

2016-02-17

Peer reviewed

IDENTIFYING PLANETARY BIOSIGNATURE IMPOSTORS: SPECTRAL FEATURES OF CO AND O₄ RESULTING FROM ABIOTIC O₂/O₃ PRODUCTION

EDWARD W. SCHWIETERMAN^{1,2,3}, VICTORIA S. MEADOWS^{1,2,3}, SHAWN D. DOMAGAL-GOLDMAN^{2,4}, DRAKE DEMING^{2,5}, GIADA N. ARNEY^{1,2,3}, RODRIGO LUGER^{1,2,3}, CHESTER E. HARMAN^{2,6,7,8}, AMIT MISRA^{1,2,3}, RORY BARNES^{1,2,3}

Draft version August 8, 2018

ABSTRACT

O₂ and O₃ have been long considered the most robust individual biosignature gases in a planetary atmosphere, yet multiple mechanisms that may produce them in the absence of life have been described. However, these abiotic planetary mechanisms modify the environment in potentially identifiable ways. Here we briefly discuss two of the most detectable spectral discriminants for abiotic O₂/O₃: CO and O₄. We produce the first explicit self-consistent simulations of these spectral discriminants as they may be seen by *JWST*. If *JWST*-NIRISS and/or NIRSpec observe CO (2.35, 4.6 μm) in conjunction with CO₂ (1.6, 2.0, 4.3 μm) in the transmission spectrum of a terrestrial planet it could indicate robust CO₂ photolysis and suggest that a future detection of O₂ or O₃ might not be biogenic. Strong O₄ bands seen in transmission at 1.06 and 1.27 μm could be diagnostic of a post-runaway O₂-dominated atmosphere from massive H-escape. We find that for these false positive scenarios, CO at 2.35 μm , CO₂ at 2.0 and 4.3 μm , and O₄ at 1.27 μm are all stronger features in transmission than O₂/O₃ and could be detected with SNRs $\gtrsim 3$ for an Earth-size planet orbiting a nearby M dwarf star with as few as 10 transits, assuming photon-limited noise. O₄ bands could also be sought in UV/VIS/NIR reflected light (at 0.345, 0.36, 0.38, 0.445, 0.475, 0.53, 0.57, 0.63, 1.06, and 1.27 μm) by a next generation direct-imaging telescope such as LUVOIR/HDST or HabEx and would indicate an oxygen atmosphere too massive to be biologically produced.

Subject headings: astrobiology—planets and satellites: atmospheres—planets and satellites: terrestrial planets—techniques: spectroscopic

1. INTRODUCTION

In recent years dozens of exoplanets have been identified that are likely or confirmed to be rocky in composition, analogous to the solar system's inner terrestrial planets (e.g., Berta-Thompson et al. 2015). Some of these known planets reside within the habitable zone (HZ) of their host star (Kopparapu et al. 2013), but are too distant from Earth for spectroscopic follow-up to characterize their planetary environments. The upcoming *Transiting Exoplanet Survey Telescope* (TESS; Ricker et al. 2014; Sullivan et al. 2015) and ground-based surveys (e.g., Charbonneau et al. 2009) will identify more nearby terrestrial HZ planets that are amenable to further study by missions such as the *James Webb Space Telescope* (*JWST*; Deming et al. 2009) or large ground-based telescopes (e.g., Snellen et al. 2013). Many of these terrestrial exoplanets will have secondary atmospheres in

which photochemistry, climate, history of atmospheric escape, volcanic outgassing, and perhaps biology will play significant roles in their atmospheric compositions (e.g., Segura et al. 2005, 2010). Understanding these star-planet interactions and geological processes will be important for characterizing a terrestrial planet's atmosphere, both to understand the planetary environment, and to increase the confidence with which we can identify planetary phenomena as being more likely to be produced by life (e.g., Des Marais et al. 2002; Segura et al. 2005; Seager et al. 2012) than by abiotic processes.

Atmospheric O₂ (or its photochemical byproduct O₃) is often considered a robust astronomical biosignature, because through the history of our planet life has been the dominant source of this gas. The exact mechanism(s) and timeline for the oxygenation of Earth's atmosphere is still under debate, but there is broad agreement on the fundamental causes (Lyons et al. 2014). The O₂ in Earth's atmosphere is unstable over geological timescales and would be depleted by reactions with reduced volcanic gases and through oxidation of the surface (Catling 2013), thus requiring an active source to maintain appreciable levels. On Earth, that active source exists in the form of photosynthetic production of O₂ by life, followed by burial of organic carbon (Catling 2013), which separates the organic carbon material from atmospheric O₂. The photochemical production of very small amounts of O₂ occurs on Earth from the photolysis of O-bearing molecules, but would not build up to appreciable levels in the absence of biology due to the shape of the UV spectrum of the Sun and significant sinks for O₂ (Domagal-Goldman et al. 2014; Harman et al. 2015).

¹ Astronomy Department, University of Washington, Box 351580, Seattle, WA 98195 USA, eschwiet@uw.edu

² NASA Astrobiology Institute's Virtual Planetary Laboratory, Seattle, WA 981195 USA

³ Astrobiology Program, University of Washington, Seattle, WA 98195 USA

⁴ NASA Goddard Space Flight Center, Greenbelt, MD 20771 USA

⁵ Department of Astronomy, University of Maryland, College Park, MD 20742 USA

⁶ Geosciences Department, Pennsylvania State University, University Park, PA 16802, USA

⁷ Pennsylvania State Astrobiology Research Center, 2217 Earth and Engineering Sciences Building, University Park, PA 16802, USA

⁸ Center for Exoplanets and Habitable Worlds, Pennsylvania State University, University Park, PA 16802, USA

The O₃ in Earth’s atmosphere is a result of photochemical reactions involving O₂, and the presence of large quantities of O₃ has been suggested as being an indicator of abundant, photosynthetically-generated O₂ (Des Marais et al. 2002; Segura et al. 2005). Recently, it has been calculated that the strongest disequilibrium indicator in Earth’s atmosphere-ocean system in terms of free energy is the N₂-O₂-dominated atmosphere coexisting with a liquid H₂O surface ocean (Krissansen-Totton et al. 2015). The common thread to all of these signatures is the presence of photosynthetically-produced O₂, and there have been many studies into the feasibility of future ground-based and space-based observations to detect O₂ spectral features in exoplanet atmospheres (e.g., Snellen et al. 2013; Misra et al. 2014a; Dalcanton et al. 2015).

Even though abiotic sources for abundant O₂/O₃ are not present for Earth, three major categories of abiotic O₂ mechanisms have been recently identified that may affect planets with different atmospheric histories or within the HZs of different types of host star. These include: 1) the photochemical production of stable concentrations of O₂/O₃ from CO₂ photolysis, which depends on the UV spectral slope of the host star and abundance of H-bearing molecules in the atmosphere (Domagal-Goldman et al. 2014; Gao et al. 2015; Harman et al. 2015; Selsis et al. 2002; Tian et al. 2014), 2) massive XUV-driven H-escape and O₂-build up on planets in the HZ during the pre-main sequence, especially for planets orbiting the latest type stars (Luger & Barnes 2015), and 3) abiotic O₂ buildup due to H-escape from N₂-poor atmospheres that lack tropospheric H₂O cold traps (Wordsworth & Pierrehumbert 2014)¹. In this work we refer to O₂ and O₃ produced by these abiotic processes as biosignature impostors. Understanding potential false positives for O₂/O₃ biosignatures is critical and timely for informing the search for life beyond the solar system, given that the first potentially habitable planets to be characterized with transmission observations will likely orbit M dwarfs, and so will be most susceptible to O₂ biosignature impostors through CO₂ photolysis and XUV-driven hydrogen escape (mechanisms (1) and (2) above).

Possible discriminators for false positive mechanisms have previously been discussed in the literature. For instance, identifying the byproducts of CO₂ photolysis using direct imaging was discussed in recent papers that described this false positive mechanism (Domagal-Goldman et al. 2014; Harman et al. 2015). N₂-depleted atmospheres without a cold trap (mechanism (3)) may be identified via the absence of pressure-sensitive N₂-N₂ CIA features (Schwieterman et al. 2015). However, previous studies have not addressed identification of CO₂ photolysis with transmission spectroscopy, or identification of the O₂-dominated atmospheres that result from massive H-escape. The O₂ abundance on Earth has self-limited to $\lesssim 0.3$ bar due to the chemical instability of higher O₂ abundances with organic matter (Kump 2008). Thus, the potentially very high O₂ pressures from massive H-loss would constitute a separate and discernible regime from biologically produced O₂ atmospheres.

Here we examine the detectability, in simulated *JWST*

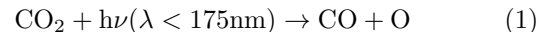
transmission spectra, of CO from CO₂ photolysis as an indicator for abiotically generated O₂/O₃ for a terrestrial HZ planet orbiting an M dwarf. We also examine the detectability of highly pressure-dependent O₂-O₂ (O₄) collisionally induced absorption (CIA) features in transmission and reflectance spectroscopy. These features would be indicators of massive, post-runaway, abiotic O₂ atmospheres. This examination builds on earlier work by (Misra et al. 2014a) that analyzed the capacity of O₄ bands to determine pressure in O₂-rich atmospheres, which were presumed to be photosynthetically generated. In §2 we describe the models used and the inputs to those models. In §3 we present the spectra of the biosignature impostor scenarios and the detectability of our proposed spectral discriminators. We discuss some of the implications of these results in §4 and present our conclusions in §5.

2. METHODS AND MODELS

2.1. Atmosphere Profiles

2.1.1. High-CO photochemical false positive

The first atmosphere scenario we consider is a habitable, but lifeless, planet with an N₂-CO₂-H₂O atmosphere, orbiting in the habitable zone of a late (M or K) type dwarf and susceptible to the abiotic accumulation of O₂ and CO through CO₂ photolysis:



Photochemically liberated O will lead to the formation of both O₂ and O₃ through the Chapman scheme, reviewed in Domagal-Goldman et al. (2014). For this scenario we use the high-O₂ case for GJ 876 from Harman et al. (2015) as our atmospheric chemical and temperature profiles (Figure 1a), as that case led to potentially detectable levels of O₂. GJ 876 is a planet-hosting M4V star with $R_* = 0.38 R_\odot$ located 4.66 pc from the solar system (von Braun et al. 2014). The modeled planet orbits at a semi-major axis of 0.15 AU. Its N₂-dominated atmosphere contains 5% CO₂, 6% O₂ and 2% CO. The temperature profile was calculated in Harman et al. (2015) by assuming a surface temperature commensurate with the stellar insolation and a moist adiabatic lapse rate to an isothermal stratosphere of 175 K. The isothermal stratosphere produces a conservative estimate of the scale height (and therefore transit depths) by neglecting short-wave heating of O₃. Isothermal stratospheres are commonly chosen in studies of abiotic O₂ generation (e.g., Domagal-Goldman et al. 2014; Tian et al. 2014) and we adopt this assumption here to be consistent with previous literature.

2.1.2. O₂-dominated post-runaway atmospheres

Luger & Barnes (2015) calculate that up to thousands of bars of abiotic O₂ can be generated by XUV-driven H-escape during the pre-main sequence phase of the planet’s host star. This depends on a number of factors, including the starting H₂O inventory (losing the H from one Earth ocean leaves behind up to 240 bars of O₂). Some of this O₂ would oxidize the surface; however we assume that there is a point where the oxidization of the planetary surface is complete and O₂ remains stable in the atmosphere. Even if geological processes slowly draw down this remaining O₂, much could remain for extended

¹ A more extensive review of oxygen "false positive" mechanisms will be presented in Meadows (2016), in prep.

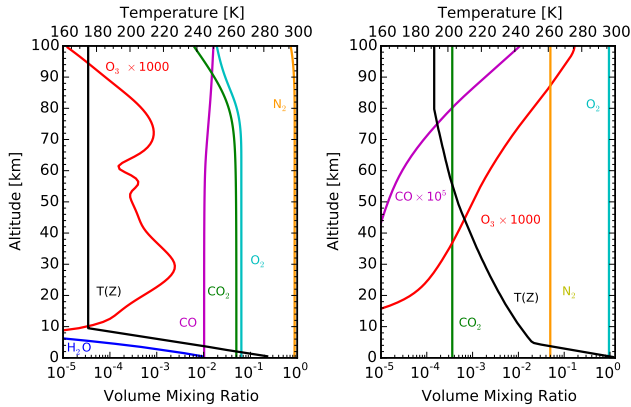


FIG. 1.— a) temperature and chemical profiles of the GJ 876 high- O_2 ($f_{O_2}=6\%$) atmosphere from Harman et al. (2015); b) temperature and chemical profiles for the O_2 -dominated ($f_{O_2}=95\%$), $P_0=100$ bar atmosphere calculated for this work.

time periods, limited by the rate of mantle overturn. Since many parameters determine how much (if any) abiotic O_2 would remain behind on these planets when they are observed, we therefore prescribe a range of surface pressures with a 95% O_2 mixing ratio: $P_0=1, 10,$ and 100 bar. The CO_2 content is similar to Earth’s, $f_{CO_2}=3.6\text{--}4$, and the rest of the atmosphere consists of N_2 and trace photochemically produced species such as CO and O_3 . To self-consistently calculate temperature and ozone profiles, we used a version of the coupled photochemical-climate model *Atmos* (Arney et al. 2016), based on photochemical and climate models originating with the Kasting group (Kasting & Donahue 1980; Segura et al. 2005; Haqq-Misra et al. 2008; Domagal-Goldman et al. 2014) and upgraded to handle high-pressure O_2 -dominated atmospheres. We assume a completely desiccated planet (no H_2O) orbiting at the inner edge of the HZ ($a = 0.12$ AU) of a star with identical properties to GJ 876. See Figure 1b for the atmospheric chemical profiles of the $P_0=100$ bar scenario.

2.2. Radiative Transfer Models and Inputs

The core radiative transfer code used for this work is the Spectral Mapping Atmospheric Radiative Transfer (SMART) model developed by D. Crisp (Crisp 1997; Meadows & Crisp 1996), which is a line-by-line, multi-stream, multi-scattering model. SMART is well-validated from data-model comparisons of Earth, Venus, and Mars (e.g., Robinson et al. 2011, 2014; Arney et al. 2014). SMART can be used to calculate synthetic direct-imaging spectra and transmission spectra using a transmission capable version of SMART that includes refraction (Misra et al. 2014a,b). All modeled spectra include O_4 absorption (O_2 - O_2 CIA), although it only produces a strong spectral impact in the cases with O_2 -dominated atmospheres. Weak O_4 bands are present in Earth’s disk-averaged spectrum (Tinetti et al. 2006; Turnbull et al. 2006). O_4 absorption has been found to be only very weakly temperature-dependent, suggesting that O_2 - O_2 CIA dominates over true van der Waals molecule absorption (Thalman & Volkamer 2013). The CIA absorption from O_4 varies quadratically with density, and the ab-

sorption coefficients can be given as:

$$\alpha(\lambda, T, d_{O_2}) = B_{O_2-O_2}(\lambda, T)d_{O_2}^2 \approx B_{O_2-O_2}(\lambda)d_{O_2}^2 \quad (2)$$

where α is the absorption coefficient, d_{O_2} is the density of O_2 molecules, and $B_{O_2-O_2}$ is a density-normalized CIA coefficient. We use the density-normalized O_4 coefficients from C. Hermans² for the 0.333-0.666 μm spectral range (Hermans et al. 1999), and the values from Greenblatt et al. (1990) and Maté et al. (1999) for the 1.06 and 1.27 μm features.

2.3. JWST NIRISS & NIRSpec noise model

We calculated the synthetic *JWST* observations as described by Deming et al. (2009) with some updates. The total throughput of the NIRISS (Doyon et al. 2014) and NIRSpec (Ferruit et al. 2014) instruments, including the telescope, were taken from Albert (2015, private communication) and from <http://www.cosmos.esa.int/web/jwst/nirspec-pce>, respectively. Thermal and zodiacal background were included as described by Deming et al. (2009), but the background only becomes significant longward of approximately 4 μm . There is very little overhead for NIRISS transit spectroscopy (Albert 2015, private communication), so we adopted an observing efficiency of unity for NIRISS. For NIRSpec, we calculated the observing efficiency assuming a 2048×32 subarray (Tumlinson 2010), and adopted a number of groups in an integration (ngrp) of 4 from Karakla et al. (2010). For both instruments, the observations are close to saturation, but we assume that saturation can be avoided by slightly dithering or scanning the telescope perpendicular to dispersion. We adopt photon-limited noise, dropping the hypothetical instrument systematic noise used by Deming et al. (2009). Recent HST experience has demonstrated close to photon-limited performance for bright stars (Kreidberg et al. 2014). We represent the star using a Phoenix model atmosphere (Allard & Hauschildt 1995).

3. SIMULATED SPECTRA OF ATMOSPHERES WITH ABIOTIC O_2

We present photochemically self-consistent test cases for two different false positive mechanisms: 1) an Earth-size planet with a prebiotic atmosphere (Figure 1a) orbiting in the HZ of GJ 876, and 2) an Earth-size planet with an O_2 -dominated (95%) 100-bar atmosphere orbiting at the inner edge of the HZ of GJ 876 (Figure 1b). These atmospheres are free of clouds and aerosols. We examine scenario (2) in transmitted and reflected light. In the reflected light case we treat GJ 876 as a stand-in for the handful of nearby late-type stars whose habitable zones may be examined with future direct-imaging telescopes such as HDST/LUVOIR (Stark et al. 2014; Dalcanton et al. 2015).

Figure 2 shows the calculated spectral transmission depths and simulated observations of case (1) in the *JWST* NIRISS (0.6-2.5 μm) and NIRSpec (2.9-5.0 μm) bands (left panel). Our calculations show that the 1.65, 2.0, and 4.3 μm CO_2 bands can be detected with a SNR > 3 (3.1, 4.3 and 8.0, respectively) when binned across the absorption bands and compared to the continuum

² <http://spectrolab.aeronomie.be/o2.htm>

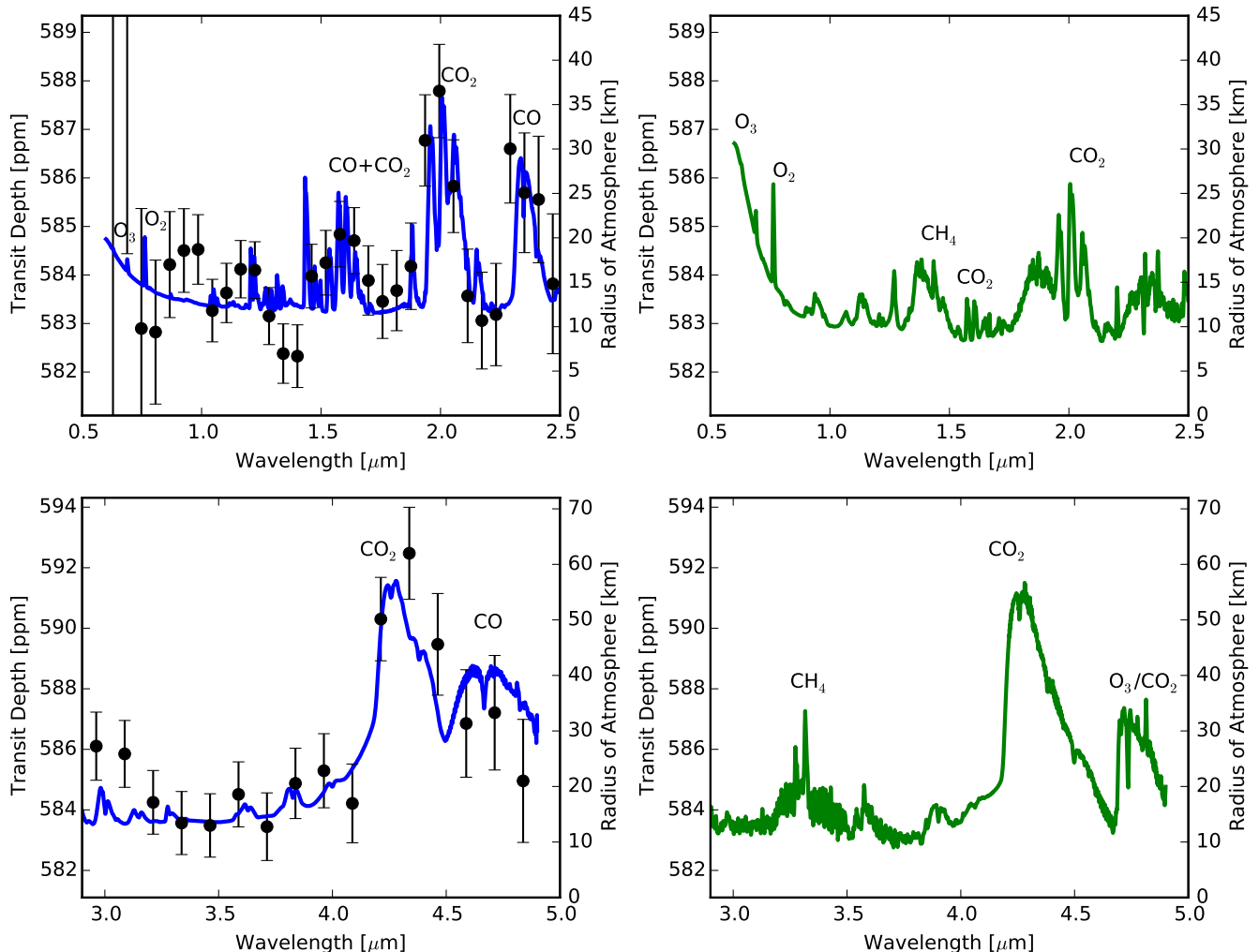


FIG. 2.— Left: Spectrum (blue) of photochemical high- O_2 /CO GJ 876 atmosphere from Harman et al. (2015) in the *JWST*-NIRISS band (top) and in the *JWST*-NIRspec band (bottom). Data points and 1σ error bars were generated with the *JWST* instrument simulator (Deming et al. 2009) assuming 65-hour integrations (10 transits of GJ 876) and photon-limited noise. Right: Comparable model spectrum (green) of Earth orbiting GJ 876 using atmosphere profiles taken from Figure 1 of Schwieterman et al. (2015).

level. The $2.35 \mu\text{m}$ CO band has a SNR of 3.7 while the $4.6 \mu\text{m}$ CO band has an SNR of 2.6. Other absorption bands have SNRs $\lesssim 1$. The simultaneous detection of both CO_2 and CO could indicate CO_2 photolysis in the planet’s atmosphere. Note that for the integration time used here, the relatively narrow O_2 -A band ($0.76 \mu\text{m}$) and weaker O_2 features would not be detectable. On the right side panel of Figure 2 we show a spectrum of modern Earth orbiting GJ 876 using atmosphere profiles from Figure 1 of Schwieterman et al. (2015), but with otherwise the same parameters as the left panel. This spectrum is not self-consistent with the star, but provided for comparison.

Figure 3 shows the calculated transmission spectrum depths of the high- O_2 atmosphere from case (2). The SNRs of the 1.06 and $1.27 \mu\text{m}$ O_4 bands are 2.8 and 3.1, respectively. The detection of strong O_4 bands would indicate a very massive O_2 atmosphere free of aerosols at high altitudes.

In Figure 4, we show simulated reflectance (direct-imaging) spectra of O_2 -dominated atmospheres ($P_0=1, 10,$ and 100 bar) seen at quadrature (solar zenith angle

of 60°) using SMART. We use the chemical profiles described in §2.1.2. For comparison we include the spectrum of an Earth atmosphere (Schwieterman et al. 2015). A gray surface albedo of $A_B = 0.15$ is assumed. The O_4 bands at $0.345, 0.36, 0.38, 0.445, 0.475, 0.53, 0.57, 0.63, 1.06,$ and $1.27 \mu\text{m}$ are labeled, with the NIR bands saturating at the highest O_2 abundance. This simple test case demonstrates that if the high- O_2 atmospheres proposed by Luger & Barnes (2015) exist, the O_4 absorption band strength in those planetary spectra would rival or exceed that of the monomer O_2 bands. These spectra are qualitatively different than modern-Earth’s spectrum, even in the $0.3\text{--}1.0 \mu\text{m}$ range, with a different shape, broader O_2 features, and additional features from O_4 . These are all signs of a much higher O_2 abundance than the Earth’s atmosphere - self-regulated by negative feedbacks - has ever achieved.

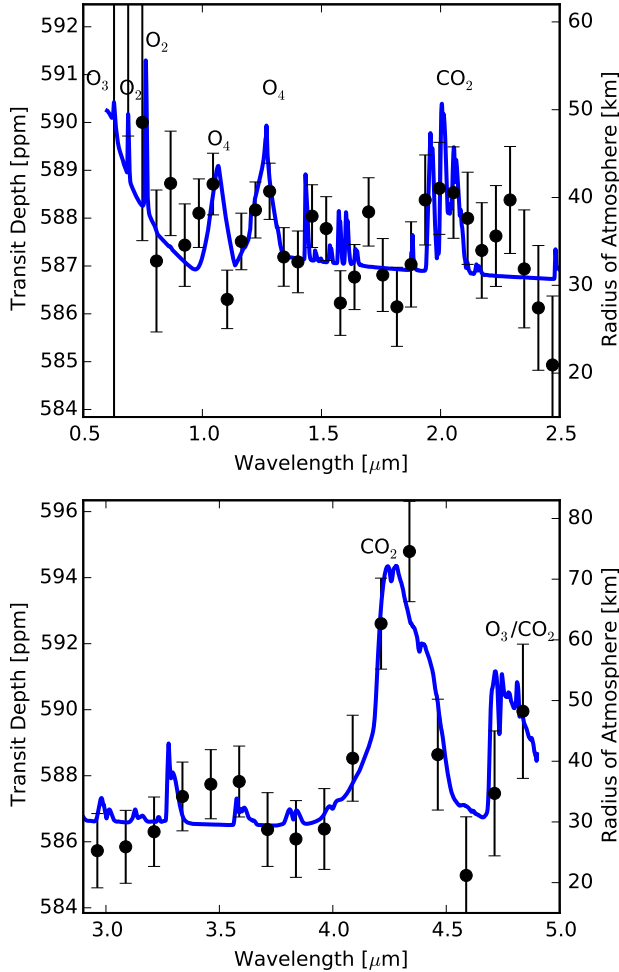


FIG. 3.— Spectra (blue) of 100 bar post-runaway O_2 atmosphere in *JWST*-NIRISS band (top) and in the *JWST*-NIRSpec band (bottom). Data points and 1σ error bars were generated with the *JWST* instrument simulator (Deming et al. 2009) assuming 65-hour integrations (10 transits of GJ 876) and photon-limited noise. See right panels of Figure 2 for a comparable Earth spectrum.

4. O_4 AND CO AS SPECTRAL INDICATORS OF ABIOTIC OXYGEN

The first potentially habitable terrestrial planet atmospheres to be characterized via transmission spectroscopy by *JWST* or large ground-based observatories will likely be orbiting near the inner edge of the HZ of late type stars (Deming et al. 2009; Sullivan et al. 2015). This is due to the detection biases of planet transit searches and the shorter orbital periods of HZ planets around late type stars, allowing greater potential to integrate over multiple transits for characterization. Unfortunately, according to current modeling studies (Harman et al. 2015; Luger & Barnes 2015) these planets are the worlds in which biosignature impostors- abiotic O_2 and O_3 - are most likely. Furthermore, this potential for false positives for life is even greater for the extended inner habitable zone for dry planets (Abe et al. 2011), which may have an even greater probability of being characterized first. The development of observing strategies to mitigate the potential for a false positive biosignature detection is thus relevant now. We argue that the detection of significant CO and CO_2 could indicate robust CO_2

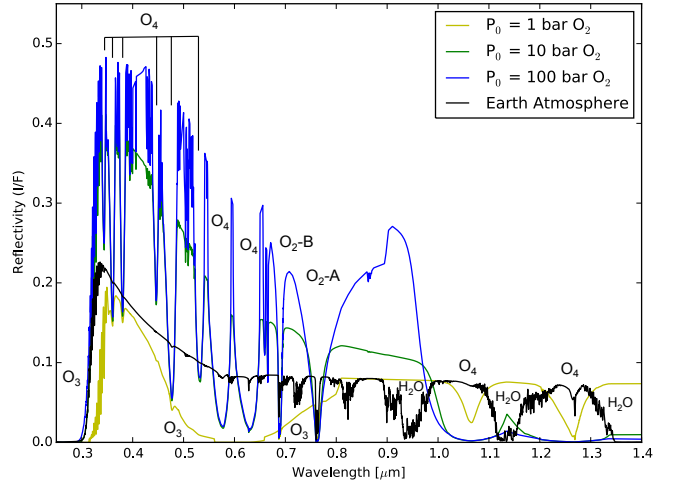


FIG. 4.— Synthetic reflectance spectra of 1, 10, and 100 bar high- O_2 atmospheres (yellow, green, and blue, respectively) with O_2 and O_4 bands identified. A comparable Earth spectrum is shown in black.

photolysis, which can produce abiotic O_2/O_3 , and also that strong O_4 bands would be indicative of an oxygen atmosphere too massive to be biological. Thus CO_2/CO and O_4 are potentially powerful spectral discriminators against abiotic O_2/O_3 in future potentially habitable exoplanet observations.

Furthermore, in the cases presented here, the spectral discriminators against abiotic O_2/O_3 are more detectable with a hypothetical *JWST* observation than the O_2 or O_3 signatures themselves. In our example spectra, neither O_2 nor O_3 would be directly detectable with just 10 transits, but the abiotic discriminators CO/CO_2 and O_4 could be. This provides an opportunity to maximize the utility of observing time if the ultimate goal is to characterize planets where true biosignatures are obtainable. If spectral indicators for biosignature impostors are detected with reasonable confidence, the community may wish to reallocate the remaining time to other promising targets, rather than integrate further. Additionally, it may also be the case that O_2 or O_3 may be identified in the same targets via other observing strategies at a concurrent or future date. For example, it has been proposed that O_2 may be found via ground-based Extremely Large Telescope (ELT) observations of the $0.76 \mu m$ O_2 -A (Snellen et al. 2013). Observations by space-based telescopes such as *JWST* or a future LUVOIR telescope operating in transit mode on a favorable target could detect or rule out these indicators before significant observing time is expended by ELTs on promising targets. If an ELT observation of a potentially habitable planet is conducted, these potential spectral discriminators could be characterized in addition to the target band (e.g., the O_2 -A band).

It is important to note that the strength of an absorption band in transmission, unlike in reflected light, is not dependent on the mixing ratio of the gas at the surface or the absolute column abundance of the gas. Rather, the strength is mostly dependent on the altitude at which the gas produces an optical depth near unity, and thus the distribution of the gas in the atmosphere is extremely important. Direct imaging of CO_2 and CO spectral signatures on an Earth twin is potentially prob-

lematic because they are weak and narrow shortward of $2.0\ \mu\text{m}$ and the planetary flux at the strongest bands (e.g., the $4.3\ \mu\text{m}$ CO_2 band) is low (Robinson et al. 2014; Schwieterman et al. 2015). Our work shows these bands are much stronger in transmission. Thus transmission spectroscopy is complementary to potential future direct-imaging characterization missions, and in particular for characterizing potential biosignature impostors. Transmission spectroscopy is also more sensitive to Earth-like CH_4 abundances than direct-imaging. Detection of CH_4 with O_2/O_3 would help confirm a true biosignature, as modeling predicts extremely low CH_4 abundances in cases of abiotic O_2/O_3 generation (Domagal-Goldman et al. 2014).

Next-generation space-based direct-imaging telescope concepts such as ATLAST/LUVOIR, HDST, and HabEx would be able to directly image planets in the HZ (Rauscher et al. 2015; Dalcanton et al. 2015; Swain et al. 2015), and thus potentially characterize biosignature gases in exoplanet atmospheres. Detection of strong O_4 bands in UV/VIS/NIR reflected light would indicate a large O_2 atmosphere originating from massive H-escape. While planets in the conservative HZ of G and F type stars would be high priority for these missions and are less susceptible to an extended history of runaway H-loss and O_2 -buildup, planets orbiting between the optimistic (recent Venus) and conservative (runaway greenhouse) inner edge of the HZ, potentially brighter targets for imaging, would also be susceptible to this process (Luger & Barnes 2015). Additionally, many nearby K and M type stars would also likely be characterized (Stark et al. 2014; Dalcanton et al. 2015), where larger regions of the HZ would be susceptible to generating biosignature impostors.

5. CONCLUSIONS

Recently proposed mechanisms for developing abiotic O_2/O_3 in terrestrial exoplanet atmospheres would produce spectral discriminators that are potentially identifiable with future telescope observations, including *JWST*. These discriminants are more detectable than O_2 or O_3 in transmission observations. CO seen at $2.35\ \mu\text{m}$ or $4.6\ \mu\text{m}$ with CO_2 at 2 or $4.3\ \mu\text{m}$ would indicate robust CO_2 photolysis and suggest a high likelihood of abiotic O_2/O_3 generation. We find that CO in a realistic exoplanet atmosphere orbiting a late type star could be seen with a $\text{SNR} > 3$ at $2.35\ \mu\text{m}$ in *JWST*-NIRISS with as few as 10 transits. O_4 bands seen in transmission or direct-imaging can be diagnostic of high- O_2 post-runaway atmospheres that have experienced a history of H-escape. The 1.06 and $1.27\ \mu\text{m}$ O_4 bands in a massive, O_2 -dominated atmosphere without high-altitude aerosols would be potentially detectable with a $\text{SNR} \gtrsim 3$ with as few as 10 transits with *JWST*-NIRISS, assuming photon-limited noise.

This work was supported by the NASA Astrobiology Institute’s Virtual Planetary Laboratory Lead Team, funded through the NASA Astrobiology Institute under solicitation NNH12ZDA002C and Cooperative Agreement Number NNA13AA93A. This research used the advanced computational, storage, and networking infrastructure provided by the Hyak supercomputer system at the University of Washington. This work made use of the NASA Astrophysics Data System. We would like to thank the anonymous reviewer for helpful comments, which improved the manuscript.

REFERENCES

- Abe, Y., Abe-Ouchi, A., Sleep, N. H., & Zahnle, K. J. 2011, *Astrobiology*, 11, 443
- Allard, F., & Hauschildt, P. H. 1995, *ApJ*, 445, 433
- Arney, G., Domagal-Goldman, S. D., Meadows, V. S., et al. 2016, *Astrobiology*, submitted
- Arney, G., Meadows, V., Crisp, D., et al. 2014, *Journal of Geophysical Research (Planets)*, 119, 1860
- Berta-Thompson, Z. K., Irwin, J., Charbonneau, D., et al. 2015, *Nature*, 527, 204
- Catling, D. C. 2013, in *Treatise on Geochemistry: Second Edition*, 2nd edn., Vol. 6 (Elsevier Ltd.), 177–195
- Charbonneau, D., Berta, Z. K., Irwin, J., et al. 2009, *Nature*, 462, 891
- Crisp, D. 1997, *Geophys. Res. Lett.*, 24, 571
- Dalcanton, J., Seager, S., Aigrain, S., et al. 2015, *ArXiv e-prints*, arXiv:1507.04779
- Deming, D., Seager, S., Winn, J., et al. 2009, *PASP*, 121, 952
- Des Marais, D. J., Harwit, M. O., Jucks, K. W., et al. 2002, *Astrobiology*, 2, 153
- Domagal-Goldman, S. D., Segura, A., Claire, M. W., Robinson, T. D., & Meadows, V. S. 2014, *ApJ*, 792, 90
- Doyon, R., Lafrenière, D., Albert, L., et al. 2014, in *Search for Life Beyond the Solar System. Exoplanets, Biosignatures and Instruments*, ed. D. Apai & P. Gabor, 3.6
- Ferruit, P., Birkmann, S., Böker, T., et al. 2014, in *Society of Photo-Optical Instrumentation Engineers (SPIE) Conference Series*, Vol. 9143, Society of Photo-Optical Instrumentation Engineers (SPIE) Conference Series, 91430A
- Gao, P., Hu, R., Robinson, T. D., Li, C., & Yung, Y. L. 2015, *ApJ*, 806, 249
- Greenblatt, G. D., Orlando, J. J., Burkholder, J. B., & Ravishankara, A. R. 1990, *J. Geophys. Res.*, 95, 18577
- Haqq-Misra, J. D., Domagal-Goldman, S. D., Kasting, P. J., & Kasting, J. F. 2008, *Astrobiology*, 8, 1127
- Harman, C. E., Schwieterman, E. W., Schottelkotte, J. C., & Kasting, J. F. 2015, *ApJ*, 812, 137
- Hermans, C., Vandaele, A. C., Carleer, M., et al. 1999, *Environmental Science and Pollution Research*, 6, 151
- Karakla, D., Beck, T., Blair, W., et al. 2010, Document JWST-STScI-002129, SM-12 (Baltimore, MD: Space Telescope Science Institute)
- Kasting, J. F., & Donahue, T. M. 1980, *J. Geophys. Res.*, 85, 3255
- Kopparapu, R. K., Ramirez, R., Kasting, J. F., et al. 2013, *ApJ*, 765, 131
- Kreidberg, L., Bean, J. L., Désert, J.-M., et al. 2014, *Nature*, 505, 69
- Krissansen-Totton, J., Bergsman, D. S., & Catling, D. C. 2015, *Astrobiology*, 16, 39
- Kump, L. R. 2008, *Nature*, 451, 277
- Luger, R., & Barnes, R. 2015, *Astrobiology*, 15, 119
- Lyons, T. W., Reinhard, C. T., & Planavsky, N. J. 2014, *Nature*, 506, 307
- Maté, B., Lugez, C., Fraser, G. T., & Lafferty, W. J. 1999, *J. Geophys. Res.*, 104, 30
- Meadows, V. S., & Crisp, D. 1996, *J. Geophys. Res.*, 101, 4595
- Misra, A., Meadows, V., Claire, M., & Crisp, D. 2014a, *Astrobiology*, 14, 67
- Misra, A., Meadows, V., & Crisp, D. 2014b, *ApJ*, 792, 61
- Rauscher, B. J., Bolcar, M. R., Clampin, M., et al. 2015, in *Society of Photo-Optical Instrumentation Engineers (SPIE) Conference Series*, Vol. 9602, Society of Photo-Optical Instrumentation Engineers (SPIE) Conference Series, 96020D
- Ricker, G. R., Winn, J. N., Vanderspek, R., et al. 2014, in *Proc. SPIE*, Vol. 9143, Space Telescopes and Instrumentation 2014: Optical, Infrared, and Millimeter Wave, 914320

- Robinson, T. D., Ennico, K., Meadows, V. S., et al. 2014, *ApJ*, 787, 171
- Robinson, T. D., Meadows, V. S., Crisp, D., et al. 2011, *Astrobiology*, 11, 393
- Schwieterman, E. W., Robinson, T. D., Meadows, V. S., Misra, A., & Domagal-Goldman, S. 2015, *ApJ*, 810, 57
- Seager, S., Schrenk, M., & Bains, W. 2012, *Astrobiology*, 12, 61
- Segura, A., Kasting, J. F., Meadows, V., et al. 2005, *Astrobiology*, 5, 706
- Selsis, F., Despois, D., & Parisot, J.-P. 2002, *A&A*, 388, 985
- Snellen, I. A. G., de Kok, R. J., le Poole, R., Brogi, M., & Birkby, J. 2013, *ApJ*, 764, 182
- Stark, C. C., Roberge, A., Mandell, A., & Robinson, T. D. 2014, *ApJ*, 795, 122
- Sullivan, P. W., Winn, J. N., Berta-Thompson, Z. K., et al. 2015, *ApJ*, 809, 77
- Swain, M. R., Redfield, S., Fischer, D. A., et al. 2015, HabX2: a 2020 mission concept for flagship science at modest cost. COPAG white paper.
- Thalman, R., & Volkamer, R. 2013, *Physical chemistry chemical physics*, 15, 15371
- Tian, F., France, K., Linsky, J. L., Mauas, P. J. D., & Vieytes, M. C. 2014, *Earth and Planetary Science Letters*, 385, 22
- Tinetti, G., Meadows, V. S., Crisp, D., et al. 2006, *Astrobiology*, 6, 34
- Tumlinson, J. 2010, Document JWST-STSci-002129, SM-12 (Baltimore, MD: Space Telescope Science Institute)
- Turnbull, M. C., Traub, W. A., Jucks, K. W., et al. 2006, *ApJ*, 644, 551
- von Braun, K., Boyajian, T. S., van Belle, G. T., et al. 2014, *MNRAS*, 438, 2413
- Wordsworth, R., & Pierrehumbert, R. 2014, *ApJ*, 785, L20